- Technical Paper -

INFLUENCE OF DRAPED EXTERNAL TENDONS ON SHEAR BEHAVIOR OF SEGMENTAL PRESTRESSED CONCRETE BEAMS

Dinh Hung NGUYEN [*1], Koji MATSUMOTO[*2], Tsuyoshi HASEGAWA[*3] and Junichiro NIWA[*4]

ABSTRACT

This paper presents the results of experimental and nonlinear finite element analysis on the segmental concrete beams with draped external tendons. The shear failure mechanism was investigated considering the effect of deviator position and inclined angle of draped tendon. The results showed that the deviator position and inclined angle of draped tendon affect deviator force and transfer force from anchorage. Shear carrying capacity of segmental concrete beams with draped external tendons was higher than that of segmental beams with straight tendons.

Keywords: segmental concrete beam, draped external tendon, inclined angle, shear mechanism

1. INTRODUCTION

Precast segmental construction is widely used in bridge structures, because of substantial cost and time saving in construction. In the beginning, internal tendon system has been used for segmental technology where tendons are located inside the concrete cross section. However, problems such as leakage at epoxy joints or corrosion in tendons may cause damage in segmental bridges. So, the application of external prestressing to precast segmental structures has been used as an innovative method in segmental concrete technology. The sudden collapse of Koror-Babeldaob bridge [1] was an example of failure of a segmental concrete bridge. Shear problem is one of probable causes, explained in Reference [1], that have been accepted to describe the collapse of Koror–Babeldaob bridge

Both straight tendon profile and draped tendon profile have been applied in a segmental concrete beam with external tendons. The difference comparing to the internal tendons is that the prestressing force from external tendons only acts on the structure at the deviators and the ends of a beam through anchorages. The draped profile has been used to alleviate congestion in anchorage zones, to reduce concrete stresses at transfer and to provide a vertical component for shear in the high shear and low moment zone in a simply supported beam. A straight external tendon profile was conducted in the author's previous study [2]. It was concluded that the effect of deviator force in a shear span on the shear capacity is insignificant. However, test data to investigate the effect of draped external tendons on the shear behavior of segmental concrete beams are very limited. Several researchers reported the experimental results focusing on the shear behavior of monolithic concrete beams with draped internal tendons [3 and 4]. Some studies focused on flexural behavior of monolithic concrete beams with draped external tendons [5]. In addition, in almost current codes the contribution of draped tendons on the shear capacity has been considered via the vertical component of prestressing force without considering the effect of location of deviators. Therefore, the effect of deviator force such as location of deviators and inclined angle of tendons on the behavior of segmental joint and shear behavior of segmental beams is necessary to be evaluated.

This paper presents experimental and nonlinear finite element analysis results of the structural behavior of segmental concrete beams prestressed with draped external tendons. The paper focuses on the response of the segmental concrete beams under the shear behavior considering the effect of draped external tendons. The inclined angle of draped tendons and the location of deviators on a shear span are main parameters. The effects of the inclined angle of draped tendons and location of deviators on a deviator force that affects the shear mechanism, such as propagation of cracks, joint opening and shear carrying capacity of segmental concrete beams are investigated.

2. TEST PROGRAM

2.1 Detail of Testing Beams

Figure 1 shows the detail of specimens in this study. Three simply supported concrete beams designed to fail in shear with a/d ratio of 3.5 were used. The distance, a_j from the loading point to the joint position in a shear span used in these beams was $1.0d$, where d was the effective depth of the beam at deviators. Test specimens were T-shaped section concrete beams with the span length of 3.2 m. The concrete stresses at the

*1 Ph.D. student, Dept. of Civil Engineering, Tokyo Institute of Technology, JCI Member
*2 Assistant Prof., Dept. of Civil Engineering, Tokyo Institute of Technology, Dr. E., JCI Member
*3 Research Engineer, Research and Development Center, DPS Bridge Works Co., Ltd.
*4 Prof., Dept. of Civil Engineering, Tokyo Institute of Technology, Dr. E., JCI Member

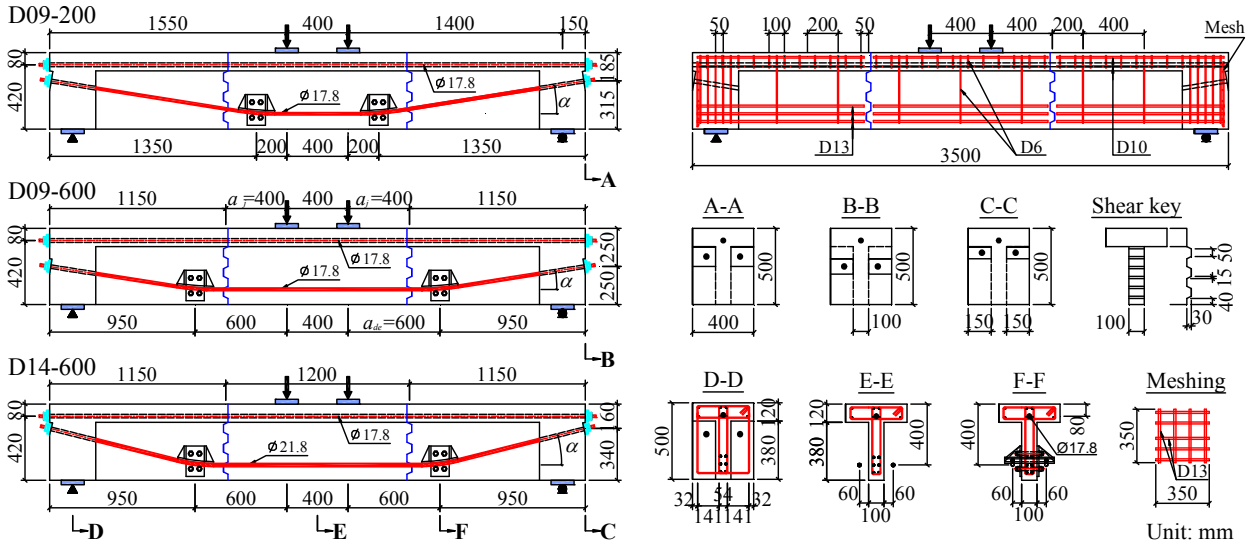

(a) General view (b) Reinforcement and Cross section

Fig. 1 Detail of specimens

Table 1 Detail of test beams

Beams	a/d	α (deg.)	a_{de} (mm)	a_j/d	Upper fiber stress, σ_u (N/mm^2)	Lower fiber stress, σ_l (N/mm^2)	Compressive strength, f'_c (N/mm^2)		Tensile strength, f_t (N/mm^2)	
							Batch A	Batch B	Batch A	Batch B
D09-200	3.5	9	200	1.0	-1.10	19.56	69.3	65.1	4.5	4.5
D09-600		9	600		-0.89	19.59				
D14-600		14.2	600		-2.00	19.21				

Note: Batches A and B are for ending segments and middle segments, respectively.

Table 2 Mechanical property of reinforcements

Bar	Yield strength (N/mm^2)	Tensile strength (N/mm^2)	Elastic modulus (kN/mm^2)	Area (mm^2)
D6	337	523	200	31.7
D10	370	524	200	71.3
D13	366	515	200	126.7

Table 3 Mechanical property of tendons

Beams	Dia. (mm)	Yield strength (N/mm^2)	Tensile strength (N/mm^2)	Elastic modulus (kN/mm^2)	Area (mm^2)
D09-200	17.8	1694	1924	191.6	208.4
D09-600	17.8	1689	1919	192.0	208.4
D14-600	17.8	1689	1919	192.0	208.4
	21.8	1649	1879	188.7	312.9

upper and lower fibers at the midspan were designed about 0 N/mm^2 and 19 N/mm^2 in compression, respectively. The inclined angle α of tendons was 9 and 14.2 deg. The location of the deviator from the loading point, a_{de} was 0.5d (200 mm) and 1.5d (600 mm). So the name of beams is D09-200, D09-600 and D14-600. Thus, D09-200 means that the inclined angle α was 9 deg. and a_{de} was 200 mm. Table 1 tabulates the tested beams and the other parameters.

2.2 Materials

The match-cast method was used for casting the segmental beams. In this method, the ending segments of each beam were cast first with a wood shear key as an end formwork. Two days later the formwork was removed and the ending segments themselves were used as the ending formworks for the middle segment in order to provide a perfect matching between the two segments. The design compressive strength of concrete, f'_c was specified as 65.0 N/mm^2 at 28 days. The actual compressive and tensile strengths of concrete are tabulated in Table 1. Epoxy resin was used to connect concrete segments. The tensile and bending strengths of the epoxy resin were about 25 N/mm^2 and 40 N/mm^2.

The arrangement of reinforcement in the beams is shown in Fig. 1(b). The non-prestressed steel bars were deformed bars. In all beams, six deformed bars with a nominal diameter of 13 mm (D13), and eight deformed bars with a nominal diameter of 10 mm (D10) were provided as internal longitudinal reinforcement at the bottom and the top flange, respectively. Deformed bars with a nominal diameter of 6 mm (D6) were used for stirrups having at an interval of 400 mm. Transverse reinforcements were also

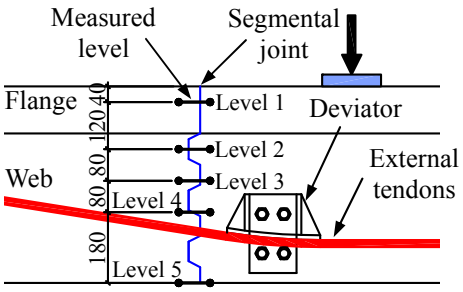

(a) Measuring joint opening in D09-200

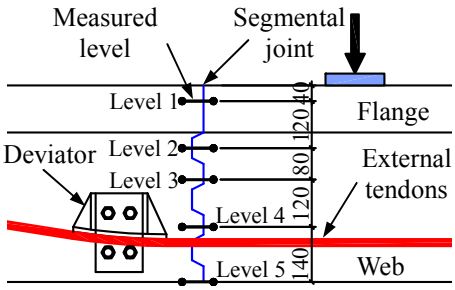

(b) Measuring joint opening in D09-600 and D14-600

Fig. 2 Measuring at 5 levels of each segmental joint

provided at the top flange with an interval of 100 mm. Meshing with D13 was utilized at the end of each beam to resist local stress due to prestressing force. The average mechanical properties of the steel bars are given in Table 2.

One unbonded internal tendon of type SWPR19L with a nominal diameter of 17.8 mm was provided in the top flange of the beams. The draped external tendons used for D09-200 and D09-600 were 19-wire type SWPR19L with a nominal diameter of 17.8 mm. The draped external tendons used for D14-600 was 19-wire type SWPR19L with a nominal diameter of 21.8 mm. The mechanical properties of the tendons are given in Table 3. The external tendons were arranged as shown in Fig. 1(a) and were stretched for four days before testing. Steel deviators were connected on the web of the beams by M22 bolts prefabricated in the web of the beams. Four Teflon sheets were provided to reduce the friction between tendon and deviator.

2.3 Loading Method and Measurements

The beams were subjected to a two-point loading test with a distance of 400 mm between two loading points as shown in Fig. 1(a). The applied load was increased monotonically by means of displacement control method.

Various measuring devices were utilized in order to measure the displacement of the beam, as well as joint opening and strain increment in the external tendons. Strain in the tendons was measured by electrical strain gauges at the middles between anchorage and deviators and at the middle of external tendons. Meanwhile, displacement transducers were mounted at the midspan, deviators and the supports of the beams to monitor the vertical deflection. At the same time, joint opening was measured at five levels on the both segmental joints of each beam, as shown in Fig. 2. Levels 1 and 2 were measured by pie-gauges while levels 3, 4 and 5 were measured by transducers.

3. RESULTS AND DISCUSSION

3.1 Generals about Testing Beams

D09-600 was first tested. For the safety, applied load was stopped when the stress in the draped lower tendons became about 1341 N/mm^2 (79 percent of the yield strength of tendons). D09-600, therefore, did not reach totally failure. D14-600 was secondly tested. The

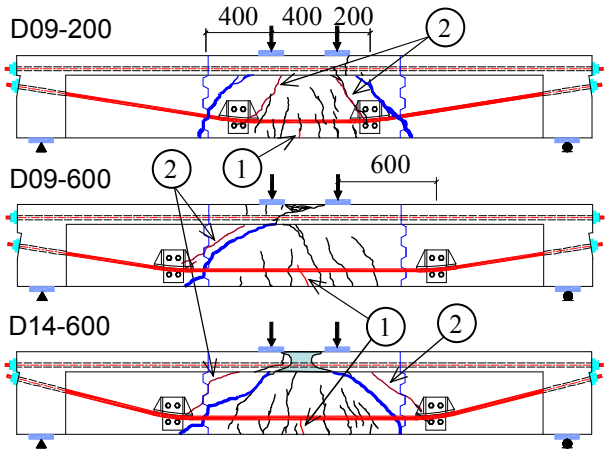

① The fist flexural crack; ② The diagonal crack from the deviator; Bold line is the dominant diagonal crack

Fig. 3 Crack patterns

applied load was provided until the beam was totally failed. D09-200 was last tested. When the stress in the draped lower tendon reached the yield strength the applied load was stopped. At the stopped load stage D09-200 had not been totally failed.

3.2 Crack Patterns

Figure 3 presents the crack pattern of the tested beams. Some flexural cracks first formed in the maximum moment zone between the loading points. Then flexural shear cracks occurred. Despite the difference in location of deviators and the inclined angle of draped tendons, one diagonal crack was observed to be formed from a deviator to the loading point. After the occurrence of diagonal cracks from deviators the dominant diagonal crack occurred at the lower corner of the segment joint toward the loading point. In D14-600 at the ultimate stage dominant diagonal crack penetrated into the top flange near the loading point. After the peak load, the crushing occurred near the loading point. In D09-200 and D09-600, before the applied load was stopped the dominant diagonal cracks were observed to penetrate into the top flange. Some cracks were seen on the top flange of a beam near the loading points. It means that these two beams, D09-200 and D09-600, were close to the ultimate state when the applied load was stopped.

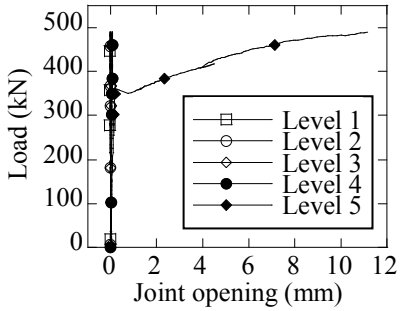

Fig. 4 Joint opening of D09-200

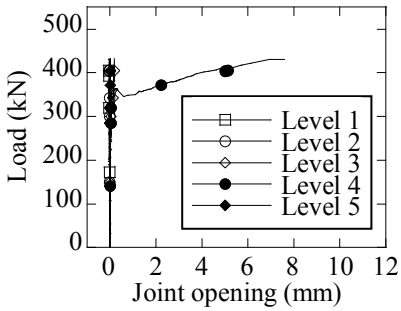

Fig. 5 Joint opening of D09-600

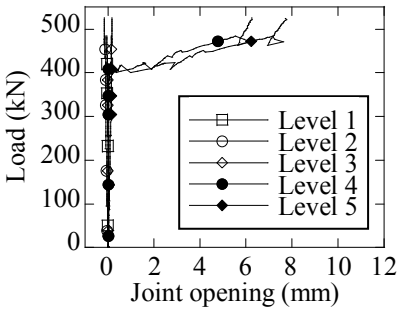

Fig. 6 Joint opening of D14-600

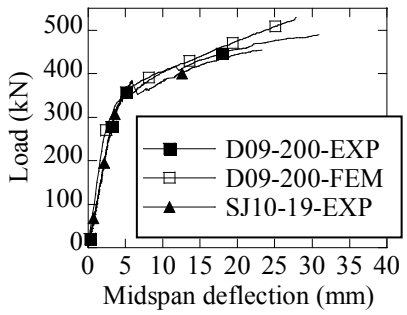

(a) D09-200

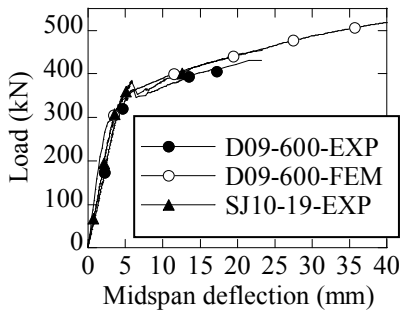

(b) D09-600

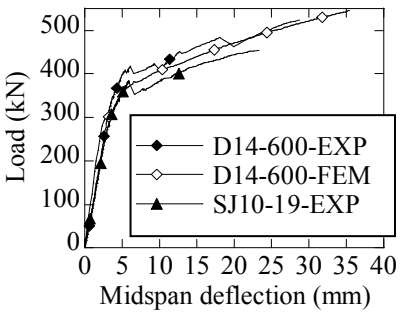

(c) D14-600

Fig. 7 Load – deflection curves

Table 4 Test results

Beams	α (deg.)	P_{cr} kN	P_{dcr} kN	P_{sh} kN	P_u kN
D09-200	9.0	280	338.4	360.2	489.2
D09-600	9.0	287.3	327.3	364.1	431.6
D14-600	14.2	285.6	408.1	417.5	523.4
SJ10-19	0	290.5	-	381.7	453.9

Note: P_{cr} is load at the first flexural crack; P_{dcr} is load at the diagonal crack formed from deviator; P_{sh} is load at the dominant diagonal crack, P_u is the peak load.

3.3 Joint Opening

Joint opening was measured at 5 levels in both segmental joints of each beam as shown in Fig. 2. Figure 4 shows the joint opening of the segmental joint on the right of D09-200. That was the critical segmental joint since larger crack width was observed in the top flange near the loading point on the right side, the joint opening of the right side was also larger. The segmental joint expressed closing the levels 1 and 2. Joint opening in the levels 3 and 4 was very small, 0.04 and 0.09 mm. Joint opening observed in level 5 where dominant diagonal crack propagated was 11.13 mm.

Figures 5 and 6 show the joint opening observed in segmental joint on the left of D09-600 and the right of D14-600 that were the critical segmental joint. The segmental joint expressed closing in levels 1 and 2 of D09-600 and D14-600. The diagonal crack from deviator was formed and passed, therefore, the level 3 joint opening of D09-600 and D14-600 was 0.28 and 0.17 mm, respectively. In the stopping load of D09-600, joint opening at level 4 was 7.57 mm. Joint opening at level 5 could not be recorded, because the failure in the lower shear key in the ending segment was occurred when the dominant diagonal crack was formed as shown in Fig. 3. At the ultimate stage of D14-600, joint opening of levels 4 and 5 was 6.25 and 7.75 mm, respectively. The joint opening of SJ10-19 in the previous test was 10.5 mm at the peak load [2].

The smaller inclined angle of tendon was, the larger joint opening was. Joint opening in D09-200 was larger than that in D09-600 and D14-600. In both D09-600 and D14-600 the joint opening did not connect between the diagonal crack from deviator and the dominant diagonal crack as shown in Fig. 3. It means that the height of opening joint was not affected by the diagonal crack from deviator.

3.4 Load-Deflection Curves and Strain Increment

Figure 7 presents the load-deflection curves of the testing beams and referred beam, i.e. SJ10-19 [2] where incline angle α was of 0 deg. Even though there was a difference of location of deviators and the inclined angle of external tendons, all the segmental beams exhibited the similar linear elastic behavior in the beginning. Linear behavior was prolonged until the first flexural crack occurred with the load, P_{cr} as tabulated in Table 4. The load of first flexural crack was affected insignificantly by the location of deviator and the inclined angle of external tendons. The load at the first flexural crack of segmental beams with draped external tendons was very close to that of the segmental beams with straight external tendons [2]. The load at the diagonal crack from deviator was not affected by the location of deviator, D09-200 and D09-600. In D14-600, higher inclined angle and area of draped external tendons, the load at the diagonal crack from

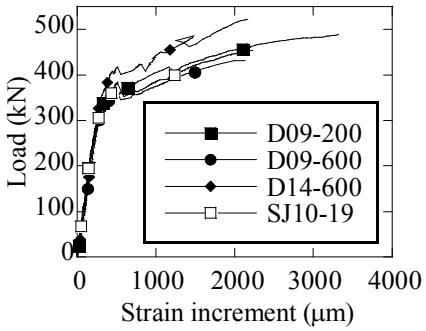

Fig. 8 Load-strain increment relationship

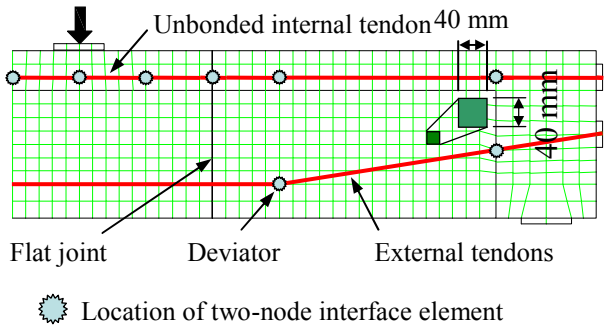

Fig. 9 A half mesh for finite element discretization

deviator was higher than that of D09-200 and D09-600. The load at the dominant diagonal crack was not affected by the location of deviator. The load at dominant crack of D14-600, higher inclined angle and area of draped external tendons, was higher than that of D09-600 and 09-200 about 13 percent. Because of stopping before failure, the maximum load of D09-600 was smaller that the ultimate load of the segmental beams with straight external tendons. The maximum load of D09-200 and the ultimate load of D14-600, however, were higher than the ultimate load of the beam with straight external tendons, SJ10-19 [2] about 8 and 15 percent, respectively.

Figure 8 illustrates the response of the strain increment in the draped external tendons at any stage of the applied load in test beams at the midspan. The tendency of the strain increment in the draped tendons was similar to that in the straight tendon. The stress increment increased small before the dominant diagonal crack. The strain increment, however, considerably increased after the dominant diagonal crack occurred.

3.5 Failure Mechanism

The linear elastic behavior of segmental beams was not affected by the location of deviator, inclined angle of draped tendons and area of external tendons. It was expressed by the load at the first flexural crack to be similar. The stiffness of segmental beams with draped tendons reduced more quickly than that with straight tendons [5] due to the second order effect. As compared with the same area of external tendons, the load at the dominant diagonal crack of segmental beams with inclined angle of 9 deg., D09-200 and D09-600, was smaller than that of the segmental beam with straight tendons, SJ10-19. However, in D14-600 with inclined angle of 14.2 deg. and higher in tendon area the loads at the diagonal crack from a deviator and the dominant diagonal crack were higher than that of D09-200 and D09-600, inclined angle of 9 deg., and straight tendon SJ10-19 as well. It means that the area of external tendons also affected the stiffness of segmental beams with draped tendons.

The crack from deviator was not formed in segmental beams with straight tendons [2 and 6]. In segmental beams with draped tendons the diagonal cracks from deviators, however, was formed before the occurrence of the dominant diagonal crack from segmental joint to the loading point. It means that deviator force was arisen and it affected the shear transfer mechanism in the segmental beams with draped tendon. The formation of the dominant diagonal crack from segmental joint to the loading point demonstrated that the local behavior of segmental joint [7] affected significantly the behavior of segmental beams. Although there was a difference in location of deviator and inclined angle of draped tendons, the shear failure mode was designated in the tested beams as the shear compression failure mode. First, the dominant diagonal crack was formed toward the loading point. Finally, the failure took place with the crushing of concrete near the loading point in the shear span. The results of this experiment show that the shear carrying capacity of segmental concrete beams with draped external tendons was higher than that of segmental beams with straight external tendons.

4. FEM ANALYSYS

4.1 Description of Models

The nonlinear finite element method (FEM) using DIANA computer program has been conducted to examine the shear mechanism with the effect of draped external tendons. The concrete beams were modeled by means of four-node quadrilateral isoparametric plane stress element as shown in Fig. 9. The behavior of concrete in compression and tension was modeled according to the model proposed by Thorenfeldt et al. [8] and Hordijk's model [9], respectively. Longitudinal reinforcements were modeled by means of the embedded reinforcement element. Tendons were modeled by a two-node truss element. The stress–strain relationship of reinforcing bars and tendons is modeled by a bilinear elasto-plastic constitutive model. The properties of concrete, reinforcing bars and external tendons are shown in Tables 1, 2 and 3.

To represent the interfacial behavior between external tendons and deviators or a concrete beam, the two-node interface element in DIANA system was applied. The stiffness of this interface element was adopted from Sivaleepunth et al. [6] in order to neglect the friction between tendons and deviators or concrete at beam ends. Two-node interface element was also provided in some positions to model unbonded internal tendon in the top flange as shown in Fig. 9.

Figure 9 also shows that the flat joint model [2] has been applied to reproduce the real geometry of joint

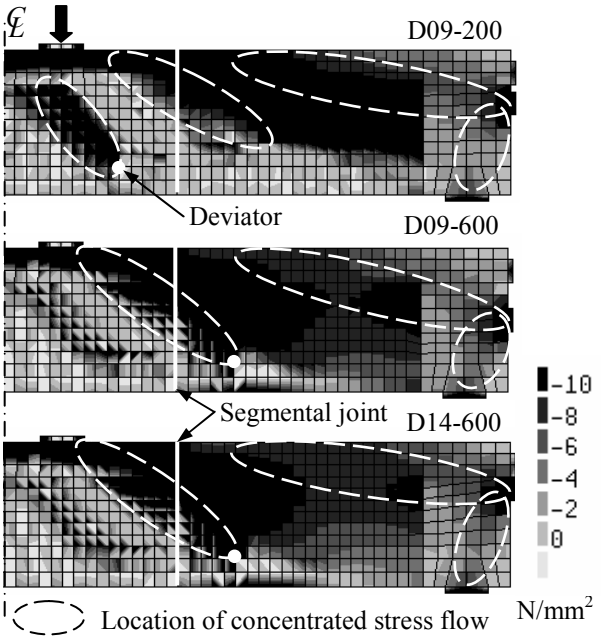

Fig. 10 Principal compressive stress at peak load

by using the two-line interface element in DIANA system. Flat joints have fewer degree of freedom which means less computer calculation time. This can be beneficial especially for complex geometries such as shear keys. The discrete crack model is selected for the interface elements of segmental joints. The normal stiffness, k_n, and tangential stiffness, k_t, in the elastic stage for flat joint model was 10^5 N/mm^3 for segmental beams with draped tendons. The tensile strength of the epoxy is higher than that of concrete. Therefore, the tensile strength of concrete, f_t was selected to model the segmental joint in the nonlinear FEM analysis.

4.2 FEM Results

In order to validate the FEM model, the results obtained from the numerical analysis were compared with the experimental results. Figure 7 also shows a good agreement of the load and deflection curves between the experimental results and FEM analysis. Figure 10 shows the principal compressive stress of all beams at the peak load. It can be seen that one concentrated stress flow formed from the deviator to the loading point. This concentrated stress flow explained the formation to the diagonal crack from the deviator to the loading point. From the anchorage there are two concentrated stress flows. One is formed from the anchorage to support. Other is tended toward the loading point. It means that not only deviator force but also the transfer behavior of prestressing force from anchorage affected the shear transfer mechanism and also the shear failure mechanism in segmental concrete beams with draped external tendons.

5. CONCLUSIONS

(1) The shear behavior of segmental concrete beams with draped external tendons was similar to that of segmental concrete beams with straight external tendons in the linear stage. After the linear stage the stiffness of segmental beams with draped tendons reduced more quickly than that with straight tendons and was affected by the area of draped tendons.

(2) The deviator force, affected by the location of deviator and the inclined angle of draped tendons, and the transfer behavior of prestressing force from anchorage affected significantly on the shear transfer mechanism of segmental concrete beams with draped external tendons.

(3) The shear compression failure mode was observed for the segmental concrete beams with draped external tendons.

(4) Shear capacity of segmental concrete beams with draped external tendons was higher than that of segmental beams with straight external tendons.

REFERENCES

[1] Burgoyne, C. and Scantlebury, R.: Lessons Learned from the Bridge Collapse in Palau, Proceedings of the ICE, Civil Engineering, Vol. 161, No. 6, pp. 28-34, 2008.

[2] Nguyen, D. H., Watanabe, K., Niwa, J. and Hasegawa, T.: Modified Model for Shear Carrying Capacity of Segmental Concrete Beams with External Tendons, Journal of Materials, Concrete Structures and Pavements, JSCE, Vol. 66, No. 1, pp.53-67, 2010.

[3] MacGregor, J. G., Sozen, M. A. and Siess, C. P.: Effect of Draped Reinforcement of Behavior of Prestressed Concrete Beams, ACI Journal, Vol. 32, No. 6, pp. 649-677, 1960.

[4] Rezai-Jorabi, H. and Regan, P. E.: Shear Resistance of Prestressed Concrete Beams with Inclined Tendons, The Structural Engineer, Vol. 64, No. 3, pp. 63-75, 1986.

[5] Tan, K. H. and Ng, C. K.: Effect of Deviators and Tendon Configuration on Behavior of Externally Prestressed Beams, ACI Journal, Vol. 94, No. 1, pp. 13-21, 1997.

[6] Sevaleepunth, C., Niwa, J., Nguyen, D. H., Hasegawa, T. and Hamada, Y.: Shear Carrying Capacity of Segmental Prestressed Concrete Beams, Journal of Materials, Concrete Structures and Pavements, JSCE, Vol. 65, No. 1, pp. 63-75, 2009.

[7] MacGregor, R. J. G., Kreger, M. E. and Breen, J. E.: Evaluation of Strength and Ductile of Precast Segmental Box Girder Construction with External Tendons, State Department of Highway and Public Transportation Research Report, No. 365-3F, Jan. 1989.

[8] Thorenfeldt, E., Tomaszewicz, A. and Jensen, J. J.: Mechanical Properties of High-Strength Concrete and Application in Design, Symposium Procceding of Utilization of High-Strength Concrete, Norway, 1987.

[9] Hordijk, D. A.: Local Approach to Fatigue of Concrete, Ph.D thesis, Delft University of Technology, 1991.